Prefulvene as a Stable Intermediate at the Potential Energy Surface Minimum of the Benzene ⇌ Benzvalene Isomerization Process

Setsuko Oikawa,* Minoru Tsuda, Yoriko Okamura, and Tadashi Urabe

Contribution from the Laboratory of Physical Chemistry, Pharmaceutical Sciences, Chiba University, Chiba 260, Japan. *Received December 12, 1983*

Abstract: MINDO/3 and ab initio calculations were carried out on prefulvene, which has been imagined as an intermediate on the isomerization path from benzene to both fulvene and benzvalene. The intrinsic reaction coordinate (IRC) on the lowest triplet state hypersurface from benzene to benzvalene revealed that prefulvene is a stable intermediate and suggested that prefulvene might be isolated or prepared under appropriate conditions. The optimized structure of prefulvene, its spin density and electron density, and the vibrational analysis were elaborated by ab initio UHF calculations with use of 3-21G and 4-31G basis sets. The benzene ⇌ benzvalene isomerization process is also discussed, determining the IRC paths on both the lowest singlet and the lowest triplet-state hypersurfaces.

Prefulvene (**1**) is imagined as an intermediate on the isomerization pathway from benzene to both fulvene and benzvalene as well as a precursor of the 1,3 cycloadduct of benzene with small alkenes.[1] There is no report, however, that **1** has been isolated or prepared. Theoretical chemistry may give some informations

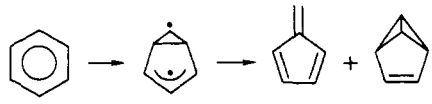

1

on the nature of this unidentified compound. In this paper, we investigate the isomerization path on the lowest triplet-state hypersurface by determining the IRC (intrinsic reaction coordinate)[2] with MINDO/3[3] calculations and find that prefulvene is an intermediate at the potential surface minimum. In order to obtain more precise informations on prefulvene, the optimized structure of prefulvene, its spin density and electron density are calculated by the ab initio UHF method with use of 3-21G[4] and 4-31G[5] basis sets. The vibrational analysis confirms both the potential surface minimum and the saddle point and gives the normal mode frequencies and zero-point energy. The benzene ⇌ benzvalene isomerization process is also discussed, determining the IRC paths on both potential energy hypersurfaces of the lowest singlet state and the lowest triplet states.

Method of Calculation

IRC (Intrinsic Reaction Coordination). The IRC is the lowest energy path connecting a reactant and a product through the saddle point on the $3N - 6$ dimensional potential energy hypersurface,[2] where N is the number of atoms constructing the reaction system. For simplicity, the IRC calculations were done on the mass-weighted $3N$ dimensional hypersurface, and then revised in such a manner so as the center of mass and the three kinds of principal axis of inertia in a structure of the reaction system are always fixed overall on the IRC path. Starting from the saddle point, the IRC path was determined point by point following the procedure proposed by Ishida et al.[6]

Geometry Optimization. Because of the difficulty of finding these points on the multidimensional hypersurface, the minima and the saddle points were determined as follows. To find the minimum point, the steepest descent path, which starts from any point on a potential energy hypersurface, was located by an IRC calculation at first. This path is called a "meta-IRC".[7] A meta-IRC leads automatically to a point which has a very small value for the norm of the energy gradient vector. Since the point reached is very close to the minimum, geometry optimization is effectively carried out by the energy gradient method[8] when this point is chosen as the starting geometry.

This procedure is very powerful for finding a saddle point. Let us consider that a rough estimation of the structure of the saddle point is the point A in Figure 1. The meta-IRC starting from A goes toward the reactant R through the point C which has the smallest value of the energy gradient vector on the meta-IRC. Suppose that another meta-IRC starting from the point B close to A goes toward the product P through D having the smallest gradient vector. The third meta-IRC going toward R, which starts from the midpoint E between C and D, gives the point G of the smallest gradient vector. The fourth meta-IRC, starting from the midpoint between E and D determines the point H of the smallest gradient vector toward P. Since the midpoint I between G and H is very close to the saddle point TS, one can decide easily the TS by the gradient method using the second derivative on the hypersurface when I is chosen as the starting geometry. The method proposed here gives a strong tool for saddle point searching compared with the direct application of the gradient method at the initial point A since the evaluation of the second derivative matrix comsumes much more computer time than that of the first derivative.

Vibrational Analysis. The vibrational analysis[9] was carried out on the mass-weighted dimensional hypersurface at both the energy minima and the saddle points.

The program for these calculations by MINDO/3 was written by the authors, and for ab initio calculations IMSPAK (Library Program of Institute for Molecular Science, Okazaki) was used without any change.

Results and Discussion

IRC on the Lowest Triplet-State (T_1) Potential Energy Hypersurface. The IRC on the T_1 state potential energy hypersurface by MINDO/3 UHF calculations is shown in Figure 2. There are two saddle points and one potential minimum. The structures

(1) D. Bryce-Smith and A. Gilbert, *Tetrahedron*, **32**, 1309 (1976), and references cited there in.
(2) (a) K. Fukui, *J. Phys. Chem.*, **74**, 4161 (1970); (b) K. Fukui, S. Kato, and H. Fujimoto, *J. Am. Chem. Soc.*, **97**, 1 (1975).
(3) R. C. Bingham, M. J. S. Dewar, and D. H. Lo, *J. Am. Chem. Soc.*, **97**, 1285 (1975).
(4) J. S. Binkley, J. A. Pople, and W. J. Hehre, *J. Am. Chem. Soc.*, **102**, 939 (1980).
(5) R. Ditchfield, W. J. Hehre, and J. A. Pople, *J. Chem. Phys.*, **54**, 724 (1971).
(6) K. Ishida, K. Morokuma, and A. Komornicki, *J. Chem. Phys.*, **66**, 2153 (1977).
(7) A. Tachibana and K. Fukui, *Theor. Chim. Acta*, **49**, 321 (1978); **51**, 189, 275 (1979); **57**, 81 (1980).
(8) J. W. McIver, Jr., and A. Komornicki, *J. Am. Chem. Soc.*, **94**, 2625 (1972).
(9) P. Pulay, "Method of Electronic Structure Theory", H. F. Schaefer III, Ed., Plenum, New York, 1977, 153.

0002-7863/84/1506-6751$01.50/0

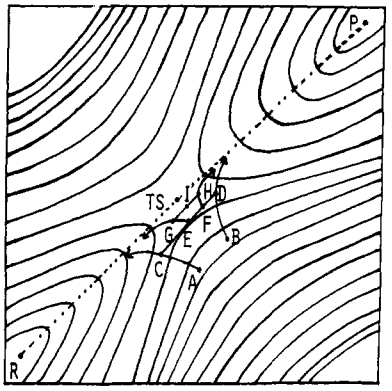

Figure 1. Procedure for finding a saddle point on the multidimensional potential energy hypersurface (see text).

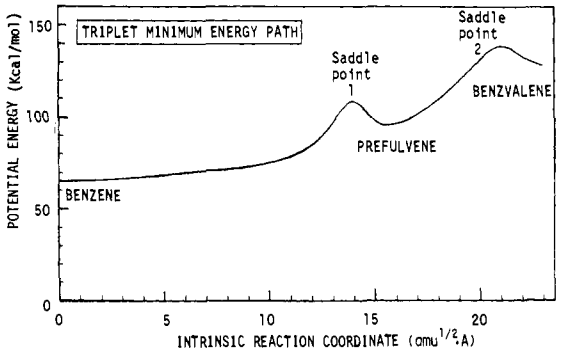

Figure 2. The T_1-IRC following the isomerization path from benzene to benzvalene (MINDO/3).

corresponding to these points were shown in Figure 3 as projections on x–y and x–z planes. Parts a and b in Figure 3 are the unique normal mode of vibration having an imaginary frequency at these saddle points. The arrows in these Figure show the displacement of each atom comprising the molecule along the reaction coordinate. The vibration of Figure 3a describes the isomerization starting from benzene to prefulvene and that of Figure 3b from prefulvene to benzvalene, respectively. The structure shown in Figure 3c is just what chemists have considered to be prefulvene. This structure having C_s symmetry appears at the minimum on the T_1 state potential energy hypersurface. The T_1 state is the ground state in this structure though the energy separation between the T_1 state and the lowest single state is very small (0.97 kcal/mol). Therefore, prefulvene might be prepared or isolated as a stable intermediate if appropriate conditions were settled in experiment.

The imaginary frequency of Figure 3a shows that prefulvene is formed from benzene in a disrotatory fashion, but C_s symmetry does not hold strictly in the saddle point. Assuming C_s symmetry, a quasi saddle point was found, which has three imaginary frequencies and whose energy is a few electron volts higher than that of the true saddle point. One of the three imaginary frequencies is a′ symmetrical in-plane vibration very similar to Figure 3a, and the others are a″ asymmetrical in-plane and out-of-plane vibrations which break C_s symmetry and lead to the true saddle point having the structure shown in Figure 3a. Therefore, the reaction path has two close branches originating from prefulvene. Jahn–Teller effect may explain the branching.

Electronic Structure of Prefulvene. The structure of prefulvene was recalculated by ab initio UHF calculations with use of 3-21G[4] and 4-31G[5] basis sets. Both ab initio calculations also supported the conclusion that prefulvene is a stable intermediate having C_s symmetry at the minimum on potential energy hypersurface of the lowest triplet state.

Ab initio calculation with the 3-21G basis set revealed that prefulvene has two configurations. One is the down-form as already shown in Figure 3c, and the other is the up-form, where the hydrogen from attached to C_1 is reversed (shown in the dotted

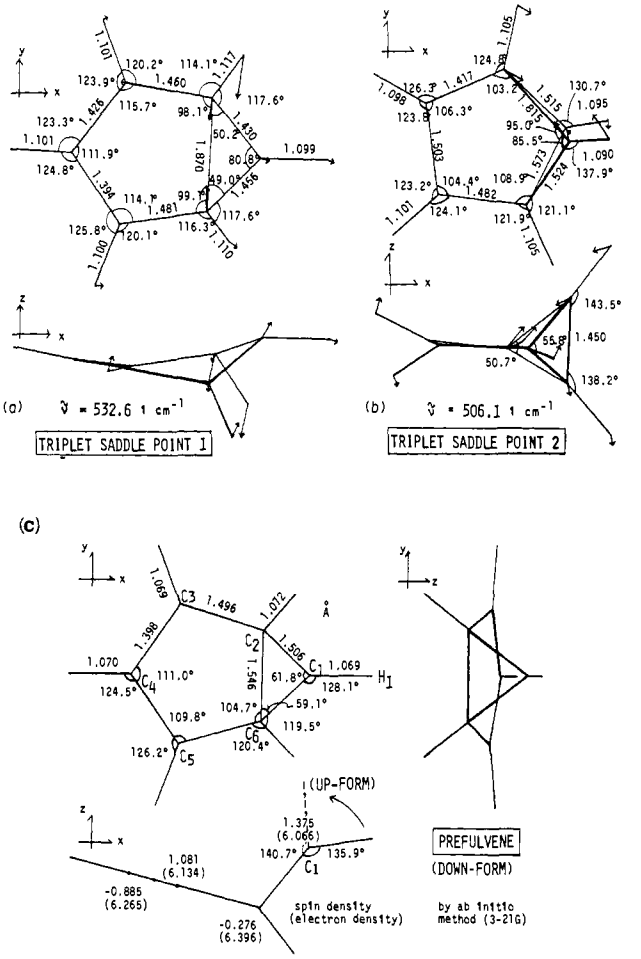

Figure 3. (a) The structure of the saddle point 1 on T_1-IRC. (b) The structure of the saddle point 2 on T_1-IRC. (c) The structure of prefulvene. Its spin density and electron density are in parentheses. The dotted line shows the up-form prevulene. Arrows in parts a and b are the normal mode of vibration of imaginary frequency which shows the structural change following the reaction coordinate from the saddle points. MINDO/3 for parts a and b. 3-21G for part c.

line in Figure 3c) and the remaining atoms occupy substantially the same position as those of the down-form. The energy level of the up-form prefulvene is 0.268 kcal/mol higher than that of the down-form. The isomerization between them easily occurs at room temperature, because the activation energy from the down-form to the up-form is 3.49 kcal/mol. At the saddle point of this isomerization process, prefulvene has such a structure that the H_1, C_1, C_2, and C_6 atoms occupy the same plane.

The total energy of prefulvene (down-form) by 3-21G level optimization is −229.27404 au. This energy is 91.3 kcal/mol higher than that for benzene and 4.40 kcal/mol higher than that for benzvalene (Table I). Figure 3c shows the optimized structure of prefulvene with its spin density and electron density. Both 4-31G and MINDO/3 level calculations give the similar results as those obtained by the 3-21G, except that MINDO/3 gives a litte longer C_2–C_6 bond length of 1.592 Å and a little shorter C_1–C_2 bond length of 1.472 Å. The large spin densities are localized on the head carbon atom C_1 in the three-membered ring, and the C_3 and C_5 atoms. The unsaturated bond is localized among C_3, C_4, and C_5 atoms in the five-membered ring. The total electron densities are almost the same on all the carbon atoms, which are negatively charged.

Molecular Orbital Correlation. The correlation diagram between the π MO's of benzene and the corresponding MO's of prefulvene is shown in Figure 4 (3-21G). The triplet ground state of prefulvene suggests that the high-energy barrier arises from HOMO–LUMO crossing on the benzene $\rightleftharpoons$ prefulvene isomerization path. As expected, there appears a HOMO–LUMO

Table I. Harmonic Frequencies and Assignments of Normal Modes of Prefulvene (C_s Symmetry)

no.	symm[a]	cm^{-1}	assignment[b]
1	A′	382	CCH bend, out of plane
2	A″	428	ring rocking
3	A′	580	ring def, out of plane
4	A′	701	ring def, out of plane
5	A″	740	ring def, out of plane
6	A′	780	ring def, in plane
7	A″	790	ring def, in plane
8	A″	826	ring open def
9	A′	833	CCH bend
10	A′	894	CC bend
11	A″	994	CC str
12	A′	1009	CCH bend, out of plane
13	A′	1041	CC str
14	A″	1089	CCH bend, CC str
15	A′	1099	CC str
16	A′	1135	CC str
17	A″	1147	CC str
18	A″	1206	CC str
19	A′	1236	CC str
20	A″	1382	CH bend
21	A′	1401	CH bend
22	A″	1415	CH bend
23	A″	1501	CH bend
24	A′	1534	CH bend
25	A′	3358	CH str
26	A′	3363	CH str
27	A′	3377	CH str
28	A′	3384	CH str
29	A′	3409	CH str
30	A′	3431	CH str

[a] Symm = symmetry species. [b] bend = bending, str = stretching, def = deformation.

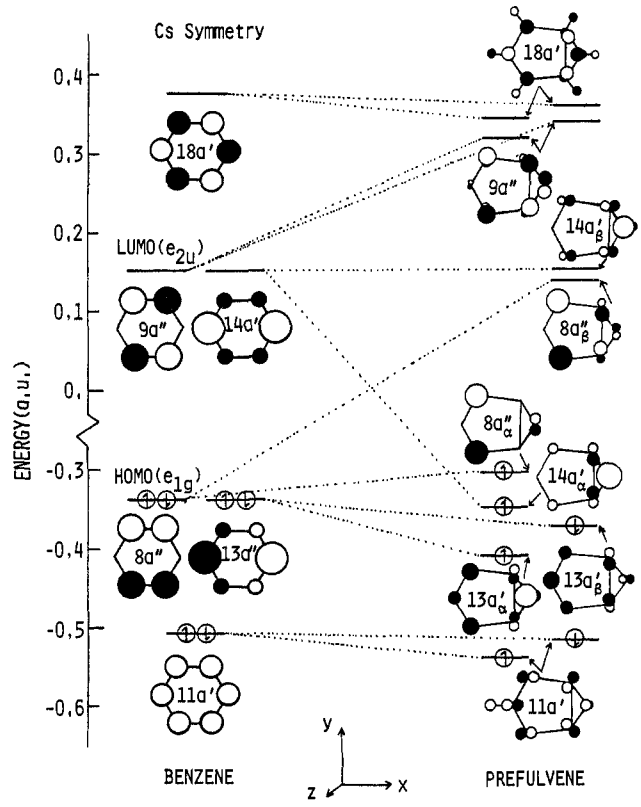

Figure 4. Correlation diagram between π MO's of benzene and the corresponding MO's of prefulvene (3-21G). α and β mean the α and β spin MO's, respectively, α and β spin MO's are substantially the same in the 18a′, 9a″, and 11a′ MO's of prefulvene. The robes of each MO in this figure are drawn by using coefficients of the orthogonalized AO, although a coefficient of a usual 3-21G MO is normalized including overlap integral. The MINDO/3 calculation gives qualitatively the same results.

crossing in the correlation diagram of Figure 4. Each of the 14a′α and 8a″α MO originating from the crossing is singly occupied by the same spin electron in ground-state prefulvene. The energy difference between these two orbitals is small (0.04455 au). This quasidegeneracy may explain the biradical property of prefulvene in the ground state. The one unpaired electron spreads mainly over the C_3 and C_5 parts in the 8a″α MO originating from the degenerated HOMO (e_{1g}) of benzene and the other over the C_1 part in the 14a′α MO originating from the degenerated LUMO (e_{2u}) of benzene. The spin density of Figure 3c originates from the electron densities of these two MO's.

From Figure 3, one can see that the bridged σ bond between C_2–C_6 of prefulvene originates from three a′ π MO's of benzene, 11a′, 13a′, and 14a′, which produce in-phase overlapping provided the reaction takes place in a disrotatory fashion. The Mulliken population analysis on the C_2–C_6 bond (Table II) elucidates more clearly the contribution of each π MO of benzene, as well as the nature of bridged C_2–C_6 bond. A positive and predominant contribution of the $2p_y$–$2p_y$ overlap population, 0.1787, to the total overlap population, 0.1709, of the C_2–C_6 bond shows that the C_2–C_6 bridge is a pure σ bond. The 14a′α MO originated from the LUMO of benzene plays the most important role on the C_2–C_6 σ-bond formation, because the contributions of the 14a′α MO for the total overlap population and the $2p_y$–$2p_y$ overlap population are 0.2063 and 0.0714, respectively, which are about 1.6 times larger than those, 0.1290 and 0.0432, of the 13a′β MO originated from the HOMO of benzene. This conclusion is quite different from Bryce-Smith's MO correlation diagram where one might imagine that the lowest π MO of benzene (11a′) is correlated to the bridged σ bond of prefulvene.[1] The 11a′α and -β MO's of prefulvene scarcely contribute to the C_2–C_6 bond formation, though the 11a′α and -β MO's have a σ character and spread all over the molecular skeleton. Three orbitals, 14a′α, 13a′α, and 13a′β, of the prefulvene originated from the two a′ π MO's (HOMO and LUMO) of benzene mainly contribute to the $2p_y$–$2p_y$ overlap population, namely the C_2–C_6 σ-bond formation. The sum of these three, 0.1289, corresponds to 72% of the total $2p_y$–$2p_y$

Table II. Mulliken Overlap Population Analysis on the C_2–C_6 Bond of Prefulvene and Benzene (3-21G)

	1,2s–1,2s[a]	1,2s–$2p_y$[b]	$2p_x$–$2p_x$	$2p_y$–$2p_y$	$2p_z$–$2p_z$	total[c]
			Prefulvene			
MO						
14a′α	0.0142	0.0762	0.0040	0.0714	0.0405	0.2063
13a′α	0.0046	0.0203	0.0056	0.0142	0.0004	0.0451
13a′β	0.0025	0.0249	0.0412	0.0432	0.0172	0.1290
11a′α	0.0050	−0.0256	0.0144	0.0247	0.0010	0.0195
11a′β	0.0053	−0.0161	0.0407	0.0095	0.0046	0.0440
sum	0.0316	−0.0797	0.1059	0.1630	0.0637	0.4439
total o.p.[d]	−0.0820	0.0880	−0.0139	0.1787	−0.0277	0.1709
			Benzene			
total o.p.	−0.0102	−0.0503	0.0031	−0.0461	−0.0070	−0.1105

[a] Sum of 1s–1s, 1s–2s, and 2s–2s atomic orbital overlap populations. [b] Sum of 1s–$2p_y$ and 2s–$2p_y$ atomic orbital overlap populations. [c] Total C_2–C_6 atomic overlap population on each MO. [d] Total C_2–C_6 atomic overlap population over all the occupied orbitals.

Table III. Total Energy of Molecules (3-21G)

molecules	total energy, au	ZPE,[a] kcal/mol
prefulvene (down-form)	-229.27404	63.56
benzene	-229.41949	68.08
benzvalene	-229.26702	
prefulvene (up-form)	-229.27362	
SP[b] (up-down isomerization)	-229.26848	
prefulvene (down-form)	-230.22830 (4-31G)	

[a] ZPE = zero-point energy. SP = saddle point.

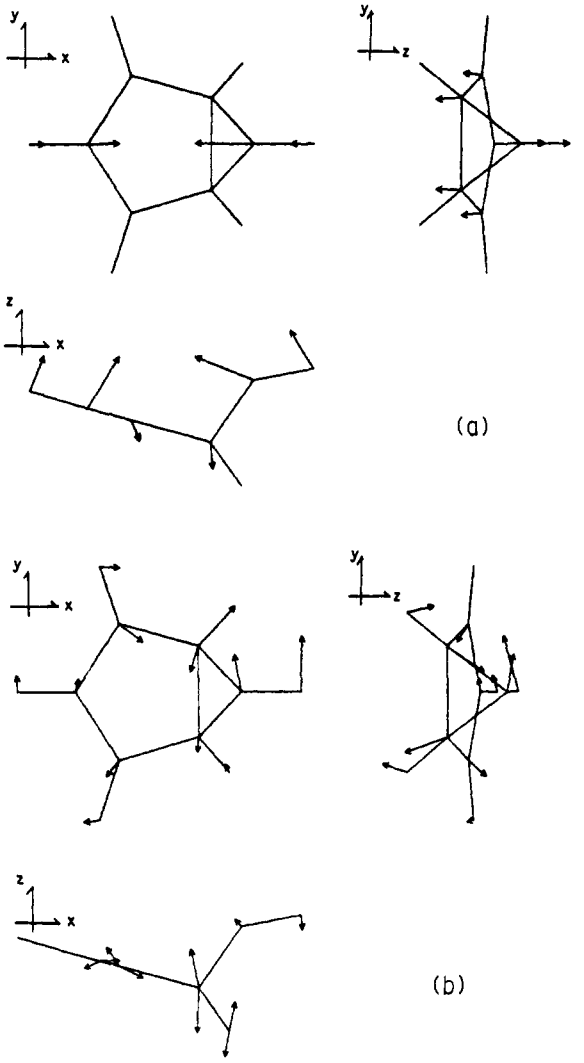

Figure 5. The normal modes of prefulvene (3-21G): (a) ν_1 and (b) ν_8.

overlap population, 0.1787, of the C_2–C_6 bond.

Vibrational Analysis. The harmonic normal mode frequencies of prefulvene are shown in Table III with the assignment of vibrations and symmetry species in the C_s point group. The calculated zero-point energy of prevulene is 63.56 kcal/mol.

The normal mode having the lowest frequency ν_1 seems to induce the isomerization between the up-form and the down-form of prefulvene as shown in Figure 5a. The eighth normal mode ν_8 is considered to initiate the three-membered ring opening which may lead to fulvene formation (Figure 5b). The characteristics of the other normal modes are briefly given in Table III. Harmonic frequencies obtained are ab initio calculations with the 3-21G basis set are always 10–15% higher than the experimental data.[4] So, one should compare the 10–15% reduced values of the data in Table III with the experimental one which may be observed in the future.

IRC on the Lowest Singlet-State (S_0) Potential Energy Hypersurface. The saddle-point geometry in benzene ⇌ benzvalene isomerization on the lowest singlet-state potential surface was

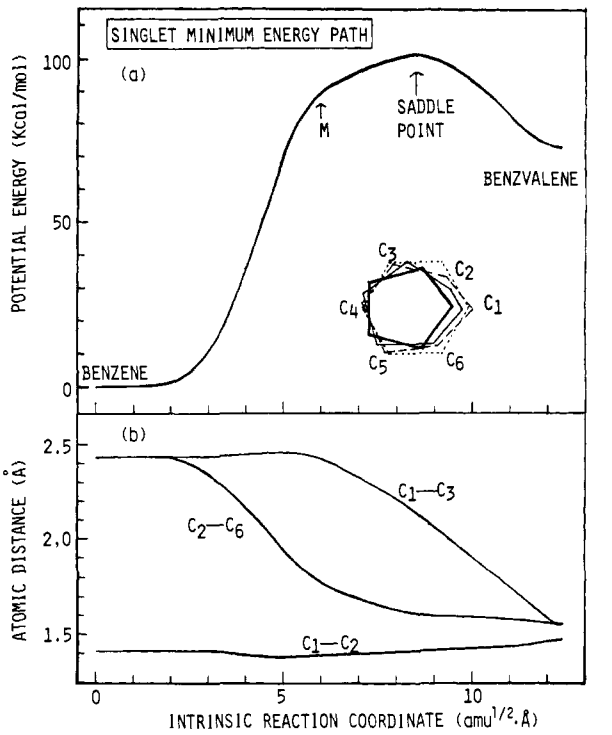

Figure 6. (a) The S_0-IRC following the isomerization path from benzene to benzvalene. (b) The atomic distance changes along the IRC (MINDO/3).

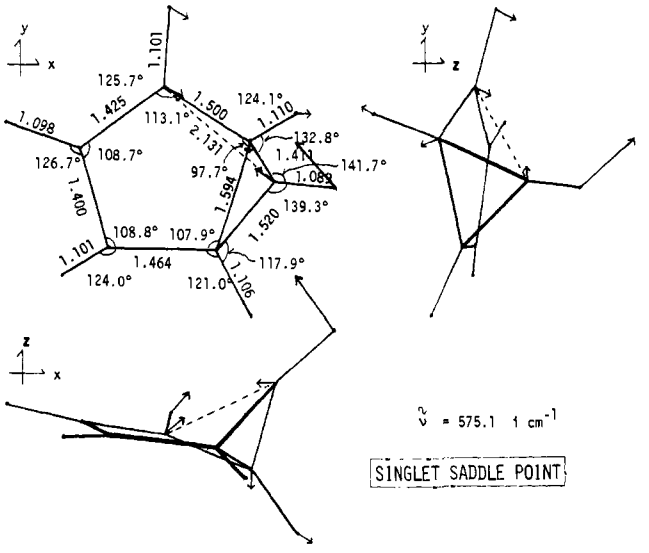

Figure 7. The structure at the saddle point on S_0-IRC. Arrows are the normal mode of imaginary frequency vibration which shows the formation of benzvalene following the reaction coordinate. The reverse side of the arrows corresponds to the benzene formation (MINDO/3).

already reported by Dewar et al.[10] However, the IRC and the imaginary vibration mode at the saddle point remain obscure. Dewar emphasized the importance of the configuration interaction (CI) calculation at the saddle-point geometry. The IRC of the isomerization on the potential energy hypersurface of the lowest singlet state (S_0) is shown in Figure 6a at the MINDO/3 level with CI which considers the 30 singly and 20 doubly excited electronic configurations.[11] The profile of the potential energy curve following the IRC is almost the same as that of the SCF calculation because the relative value of the potential energy is unchanged by CI throughout the IRC route.

(10) M. J. S. Dewar and S. Kirschner, *J. Am. Chem. Soc.*, **97**, 2932 (1975).
(11) M. Tsuda and S. Oikawa, *Photogr. Sci. Eng.*, **23**, 177 (1979).

The structure of the saddle point is shown in Figure 7 with the unique normal mode of vibration having an imaginary frequency. The vibration describes well the formations of benzvalene, if one follows the direction of the arrows of vibration in Figure 7, and benzene, if one imagines the reverse directions of the arrows. The changes of atomic distances following the rearomatization are shown in Figure 6b. Starting from benzvalene on the IRC route, the structural change appears in the C_1–C_3 bond dissociation at first. Thus, the molecule does not hold any of the C_s or C_2 symmetry overall on the IRC route from benzvalene to benzene. Although the thermal isomerization appears to be a one-step reaction on the S_0 potential energy hypersurface of Figure 6a, precise examination of the bond lengths of Figure 6b reveals that the reaction proceeds in two steps.

In contrast to the IRC on the T_1 hypersurface, the IRC on the S_0 hypersurface does not go through the point corresponding to the prefulvene structure. The point nearest to prefulvene on the S_0 hypersurface is shown as M in Figure 6a, where the C_1–C_3 bond is fully loosened and the C_2–C_6 bond is as tight as prefulvene. The prefulvene structure is not a minimum on the S_0 hypersurface, and the steepest descent path from the prefulvene structure leads directly to benzene.

The rearomatization of benzvalene may proceed mainly through the IRC route shown in Figure 6a. So, prefulvene will not be produced in the thermolysis of benzvalene. Because of the singlet–triplet intersection around the prefulvene structure, a chemiluminescence is expected if prefulvene is produced in the rearomatization path from benzvalene to benzene. In the analogous rearomatization of Dewar benzene to benzene,[12,13] an energy transfer from triplet-state benzene, which is produced in the thermolysis, to 9,10-dibromoanthracene was followed by the fluorescence of the latter.[14] Turro et al.,[15] however, reported that no chemiluminescence was observed in the thermolysis of benzvalene.

Acknowledgment. The authors thank the Computer Center, Institute for Molecular Science, Okazaki, for the use of the M-200H computer and the Library program IMSPAK. The computation was carried out, in considerable part, at the Computer Centre, the University of Tokyo, and the Computer Center, Chiba University. This work was supported in part by Grant in Aid for Scientific Research No. 58209009 from the Ministry of Education, Science and Culture.

Registry No. 1, 81181-42-2; benzene, 71-43-2; benzvalene, 659-85-8.

(12) M. J. S. Dewar, S. Kirschner, and H. W. Kollman, *J. Am. Chem. Soc.*, **96**, 7579 (1974).
(13) M. Tsuda, S. Oikawa, and K. Kimura, *Int. J. Quantum Chem.*, **18**, 157 (1980).
(14) N. J. Turro, P. Lechtken, G. Schuster, J. Orell, H. C. Steinmetzer, W. Adam, *J. Am. Chem. Soc.*, **96**, 1627 (1974).
(15) N. J. Turro, C. A. Renner, T. J. Katz, K. B. Wiberg, and H. A. Connon, *Tetrahedron Lett.*, **46**, 4133 (1976).

Partitioning of Orbital Framework in Dibenzotetracene Dianion: Manifestation of the Role of Antiaromaticity in $4n\pi$ Conjugated Systems

Abraham Minsky and Mordecai Rabinovitz*

Contribution from the Department of Organic Chemistry, The Hebrew University of Jerusalem, Jerusalem 91904, Israel. *Received December 27, 1983*

Abstract: The twofold reduction of dibenzotetracene (**1**) to its corresponding dianion was performed with lithium and sodium metals. The resultant doubly charged species revealed unusual ^{1}H NMR patterns which indicate the existence of a partitioning of the MO's framework of $\mathbf{1}^{2-}$ into two parts: "anthracene"-like and "phenanthrene"-like systems, each system exhibiting independent characteristic features, similar to those observed in anthracene and phenanthrene dianions. This mode of partitioning of the condensed system as well as features revealed by the 9-(9′-phenanthryl)anthracene (**4**) tetraanion seem to be an outcome of the imposed antiaromatic contributions.

The term "aromaticity" represents a basic, inherent difficulty related to the fact that the aromatic character is not physically observable and hence cannot be directly expressed by measurable data. Still, the notion of aromaticity serves a useful purpose as it enables a general interpretation of a large variety of structural, chemical, and physical phenomena.

The hurdles to be passed in a discussion of the concept of antiaromaticity are even higher, as the experimental data related to the antiaromatic character are quite limited. In principle, cyclic or polycyclic conjugated systems of $4n\pi$ electrons in their peripheral path of conjugation are expected to reveal antiaromatic contribution.[1] Yet, in most cases these contributions, being unfavored in terms of Hückel's rule, are minimized by various mechanisms which reduce the efficiency of the $4n\pi$ electron cyclic delocalization. Antiaromaticity as well as the mechanisms which act to quench its manifestation may account for some highly unexpected phenomena which occur in systems where the antiaromatic property is imposed by virtue of the "anti-Hückeloid" number of π electrons. This contribution is concerned with the crucial roles which antiaromaticity seems to display in $4n\pi$ conjugated polycycles, a role vividly demonstrated by these phenomena.

(1) (a) Breslow, R. *Acc. Chem. Res.* **1973**, *6*, 393–398. (b) Haddon, R. C.; Haddon, V. R.; Jackman, L. M. *Fortschr. Chem. Forsch.* **1970**, *16*, 103–220. (c) Cox, R. H.; Terry, H. W.; Harrison, L. W. *Tetrahedron Lett.* **1971**, *50*, 4815–4818.

Results and Discussion

Dibenzotetracene (1) Dianion. The reduction of dibenzotetracene (**1**) to its corresponding hitherto unknown dianion was performed by lithium and sodium metals. The deep purple

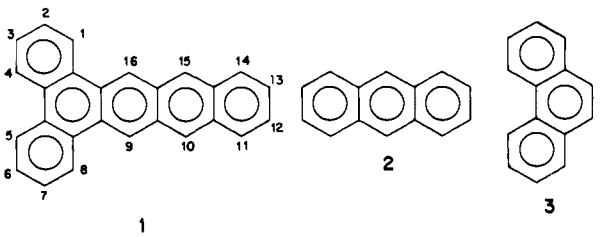

0002-7863/84/1506-6755$01.50/0